ACS APPLIED MATERIALS & INTERFACES

Research Article

www.acsami.org

Inkjet-Assisted Layer-by-Layer Printing of Encapsulated Arrays

Rattanon Suntivich, Olga Shchepelina, Ikjun Choi, and Vladimir V. Tsukruk*

School of Materials Science and Engineering, Georgia Institute of Technology, Atlanta, Georgia 30332-0245, United States

Supporting Information

ABSTRACT: We present the facile fabrication of hydrogen-bonded layer-by-layer (LbL) microscopic dot arrays with encapsulated dye compounds. We demonstrate patterned encapsulation of Rhodamine dye as a model compound within poly(vinylpyrrolidone)/poly(methacrylic acid) (PVPON/PMAA) LbL dots constructed without an intermediate washing step. The inkjet printing technique improves encapsulation efficiency, reduces processing time, facilitates complex patterning, and controls lateral and vertical dimensions with diameters ranging from 130 to 35 μm (mostly controlled by the droplet size and the substrate hydrophobicity) and thickness of several hundred nanometers. The microscopic dots composed of hydrogen-bonded PVPON/PMAA components are also found to be stable in acidic solution after fabrication. This facile, fast, and sophisticated inkjet encapsulation method can be applied to other systems for fast fabrication of large-scale, high-resolution complex arrays of dye-encapsulated LbL dots.

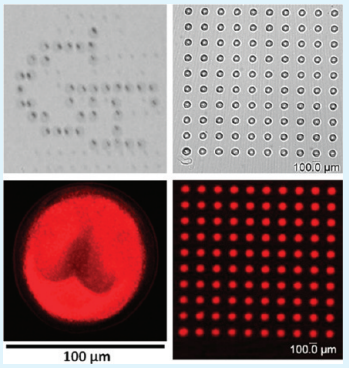

KEYWORDS: *inkjet printing, encapsulation, patterning, layer-by-layer assembly, hydrogen bonding, thin film*

INTRODUCTION

Ultrathin functional polymer films, micropatterned arrays, and microcapsules are important for diverse applications in sensing, catalysis, cell culture, and drug delivery.[1,2] Layer-by-layer assembly (LbL) is one of the prominent techniques which can be used to create such materials and structures with controlled thicknesses, morphology, diverse functionalities, and unique structures.[3,4] LbL component selection might include regular polyelectrolytes, dendrimers, proteins, nanoparticles, colloids, and biomaterials.[5−16] Further tailoring of LbL multilayer structures, beyond uniform films and spherical microcapsules, for demanding applications is focused on the adaptation of such advancements in the known nanotechnologies such as inkjet printing, microcontact printing, micromolding, and dip-pen nanolithography.[17−25] These approaches allow for the facile fabrication of patterned LbL structures with controlled spatial configurations which have multicompartment periodic patterned structures at different length scales.

However, despite significant progress, the formation of discrete LbL structures with controlled shapes and a periodic spatial arrangement of components in large arrays remains a challenge while using conventional dip, spin, and spraying methods.[26,27] On the other hand, the inkjet printing technique, which utilizes microdroplet deposition via a microscopic nozzle, can be considered a facile and powerful top-down route for creating complex arrays when combined with bottom-up LbL assembly. Accordingly, inkjet printing-assisted LbL multilayer assembly is expected to yield well-defined micropatterned structures with nanometer thickness and microscopic lateral dimensions. Using inkjet printing enabled manipulation of the drop size, location, and speed to fabricate the complex dot arrays according to a preprogrammed automatic process.[17,28,29] The uncontrolled spreading of liquid droplets on solid substrates following impact and dewetting processes due to a mismatch in surface energy might compromise the printing resolution due to, e.g., coffee ring formation during the drying process. Droplet spreading is a common issue complicating this technique, and its effect can be mitigated by controlling the distance between substrate and nozzle, viscosity of the ink solution, evaporation rate, and the use of a suitable primer coating on the substrate. To increase the speed of the deposition process, rapidly drying layers of minute thicknesses are used which helps prevent a deviation from the initial shape during multiple deposition cycles. Well-aligned microprinting processes lead to minimized deviation from a targeted center during the multiple repetition of droplet deposition and thereby builds LbL structures with microscopic precision. The size of the polymer droplets can be further reduced with the assistance of an electric field, down to a few hundred nanometers in diameter.[30]

Several examples of applying inkjet printing for LbL film formation from different pairs of polyelectrolytes with hydrogen and ionic interactions have recently been demonstrated.[31,32] In these studies, the authors demonstrated that inkjet-assisted LbL assembly can be indeed utilized to fabricate large scale uniform ultrathin films and micropatterns with a typical resolution in the range of 100−300 μm. It has been suggested that even higher spatial resolution can be achieved by reducing the nozzle dimensions, viscosity of solution, and liquid spreading.[33] These parameters can be used to build patterns with complex compositions. However, very little has been

Received: March 13, 2012
Accepted: May 7, 2012
Published: May 8, 2012

   dx.doi.org/10.1021/am3004544 | ACS Appl. Mater. Interfaces 2012, 4, 3102−3110

Scheme 1. Inkjet-Assisted LbL Printing and Encapsulation with Idealistic Schematics of Multilayered Inner Dot Morphologies[a]

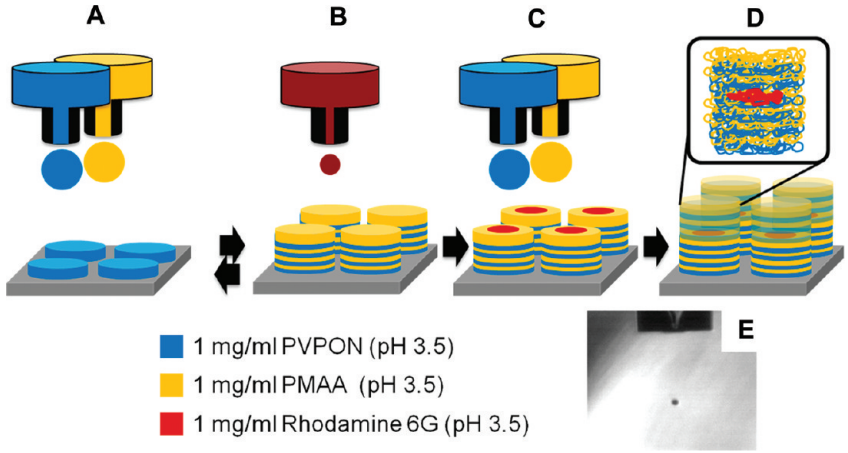

[a](A) Formation of LbL dot, (B) rhodamine dye loading, (C) formation of capping film, (D) dye-encapsulated array (the inset indicates an idealized schematics of multilayered film), and (E) an optical image of a PVPON droplet injected from a 50 μm nozzle.

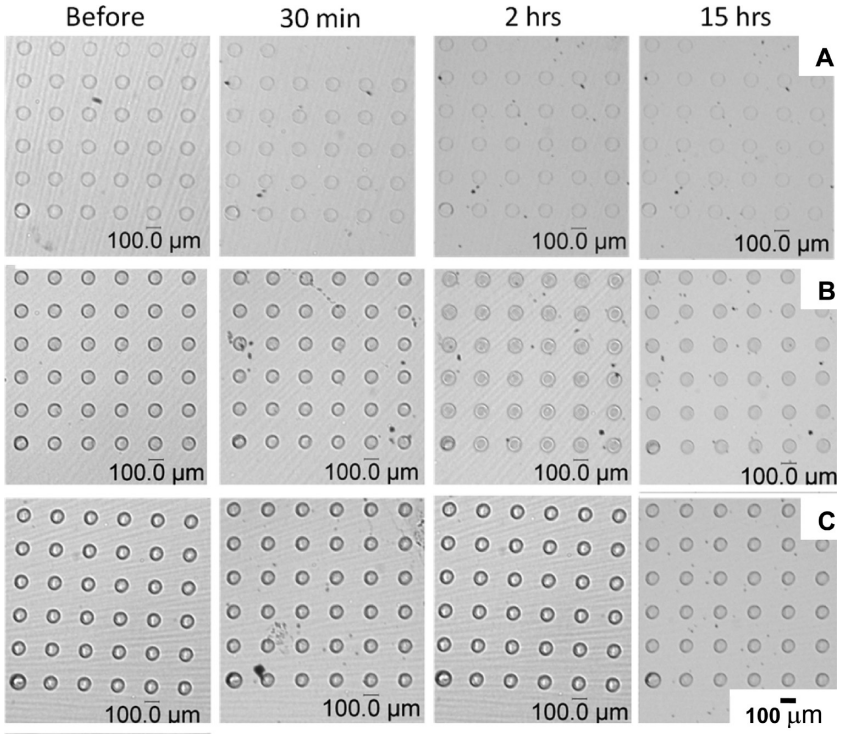

Figure 1. Optical microscopic images demonstrate the LBL dot array with different exposure times in buffer with pH 3.5: (A) 1 bilayer, (B) 3 bilayers, and (C) 5 bilayers.

published to date on high-resolution micropatterned composite LbL arrays via inkjet-assisted LbL assembly.

Here, we report on the fabrication of higher-resolution and large scale arrays of LbL dots with encapsulated fluorescent dye via facile inkjet-assisted LbL assembly without a rinsing step. The model dye compound, Rhodamine 6G, was efficiently encapsulated within pH responsive hydrogen-bonded robust poly(vinylpyrrolidone)/poly(methacrylic acid) (PVPON/PMAA) LbL dots. Microscopic LbL dots around 100 μm in diameter were fabricated with different numbers of bilayers ranging from 2 to 10 with the thicknesses between 50 and 500 nm. Moreover, we achieved higher spatial resolution with LbL dot diameter decreasing to below 40 μm by applying microprinting with the narrowest nozzle and limiting droplet spreading on highly hydrophobic substrates.

EXPERIMENTAL SECTION

Materials. Poly(vinylpyrrolidone) (PVPON; molecular weight (MW) = 40 kDa), poly(4-vinylphenol) (PHS, MW = 25 kDa), Rhodamine 6G Dye (95% purity), hydrochloric acid, sodium hydroxide, and dibasic and monobasic sodium phosphate were purchased from Sigma-Aldrich. Polystyrene (PS, MW = 250 kDa) and toluene were purchased from Janssen Chimica and J.T. Baker, respectively. Poly(methacrylic acid) (PMAA; MW = 100 kDa) was purchased from PolyScience. All chemicals were used without further modification. Nanopure water (Barnstead) with an 18.2 MΩ·cm resistivity was used for all experiments.

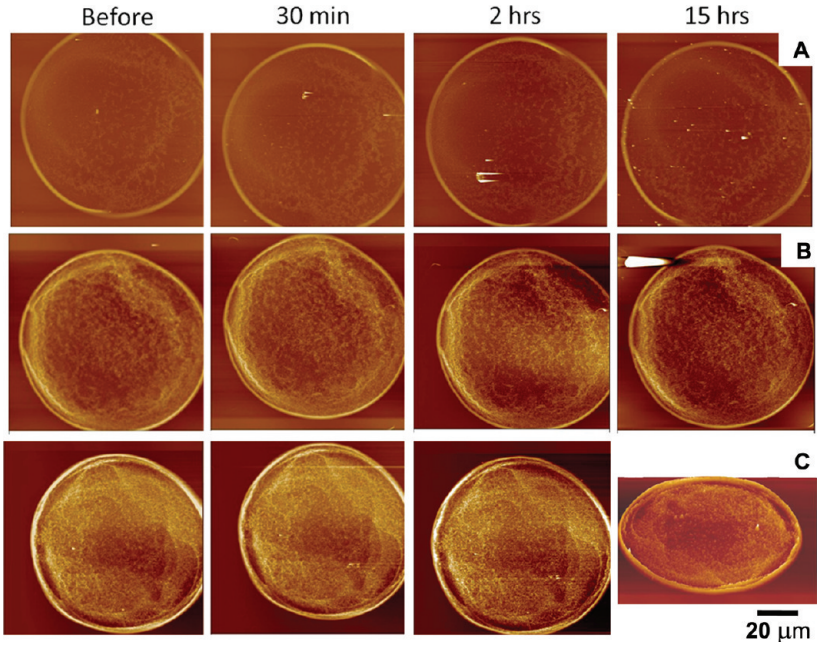

Figure 2. AFM images of LBL dot with different exposure times in buffer pH 3.5: (A) 1 bilayer, (B) 3 bilayers, and (C) 5 bilayers. The bottom right image in (C) is a 3-D image of a 5 bilayer LbL dot after expose to buffer for 15 h. The image size is 100 μm for all images. The height is 500 nm for all AFM images and 2 μm for a 3-D AFM image.

Silicon substrates were cut into 1 × 2 cm^2 pieces from 3 in. diameter wafers (University Wafer). Piranha solution (3:1 concentrated sulfuric acid and hydrogen peroxide mixture) was used to clean the substrate according to the normal procedure used in our laboratory (*warning: hazardous solution*).[34−36] The silicon substrates were rinsed with Nanopure water and dried under dry nitrogen. Glass cover slides were purchased from VWR and used as received. For the preparation of hydrophobic substrates, either a 2 wt % PHS or 2 wt % PS solution was dissolved in dioxane or toluene, respectively, and spun cast at 3000 rpm onto the glass slide for 30 s.

Fabrication and Characterization. Inkjet-assisted LbL printing was conducted by adjusting the pH condition of a 1 mg/mL PVPON solution to pH 3.5 and printing the polymer solution on a glass substrate both with and without a polymer coating. A 1 mg/mL PMAA solution at pH 3.5 was printed at the same positions on top of the PVPON layer in order to form a single bilayer. The printing process was repeated by following these steps to fabricate LbL dots of varying thickness. Intermediate rinsing steps, otherwise common in LbL fabrication, were not used in these inkjet-printing processes. A JetLab II inkjet printer (MicroFab Technologies) was used for experiments with 50 μm nozzle diameters for printing PVPON/PMAA dots and 20 μm nozzle for deposition of Rhodamine dye. The printing speed was around 100 dots per 30 s without intermediate drying steps.

Encapsulation of fluorescent dye into LbL dots was achieved by first fabricating 1, 3, or 5 bilayers followed by the addition of Rhodamine 6G deposited from an independent nozzle in the middle of the existing polymer bilayer dot structure (Scheme 1). The dot was then capped with 1, 3, or 5 LbL bilayers. Arrays of LbL dots with encapsulated fluorescent dye between a different number of bilayers were formed: 2 bilayers (1 + 1 bilayer), 6 bilayers (3 + 3 bilayer), and 10 bilayers (5 + 5 bilayers). The pattern used for printing was uploaded from a monochromatic (black and white) bitmap file. The white pixels denoted "print" areas whereas the black areas were "do not print" areas and were uploaded to the JetLab II program prior to use. The number of pixels controlled the size of the pattern and the distance between the printed dots both on the *x*- and *y*-axis. The maximum speed of operation was 900 Hz, and number of LbL dots was 100.

The surface morphology of the arrayed LbL dot was characterized by atomic force microscopy (AFM). The AFM images were obtained using a Dimension 3000 AFM microscope (Digital Instruments) under a "light" tapping mode regime according to standard procedures.[37,38] The samples were scanned at 100 μm × 100 μm, 20 μm × 20 μm, and 5 μm × 5 μm scan sizes using triangle cantilevers with resonance frequencies near 330 kHz and spring constants of 40 N/m (MikroMasch). A fluorescent microscope (DM 4000M, Leica) was used to investigate the overall stability and patterning performance of the LbL arrays before and after encapsulation of Rhodamine dye.

RESULTS AND DISCUSSION

Inkjet printing was conducted on different hydrophilic and hydrophobic substrates including hydrophilic (glass, silicon) and hydrophobic (PHS, PS) substrates. Optical images in Figure 1 demonstrate a 6 × 6 dot array with different numbers of LbL bilayers printed on a PHS substrate. LbL dots printed on PHS and PS surfaces will be the primary focus of this work since the hydrophobic surface allows a higher resolution printing process than that on glass or silicon substrates. The hydrophobic surfaces prevent the spreading of the liquid droplets after impact, allowing it to remain confined to a single area with better resolution (Figures S1 and S2, Supporting Information).

The droplet diameter during deposition under optimized conditions with a 50 μm nozzle was around 45 μm (Scheme 1E and Figure S3, Supporting Information). However, the average diameter of the LbL dots on PHS substrate was around 90 μm due to the fast spreading behavior of the polymer solutions during impact event (Figures 1 and 2). Such a large spreading indicates a high Weber number which is common for inkjet-assisted deposition.[39]

The diameter of the LbL microdots remain virtually constant for different numbers of LbL bilayers and varies from 95.7 ± 1.8 μm for 1 bilayer dots to 87.9 ± 1.1 μm for 5 bilayer dots. We suggest that this consistency in dimension is due to the restriction of solution spreading on the hydrophobic polymer surface, even after multiple repetitions of LbL deposits. A PVPON droplet deposited on a PHS substrate forms a coffee ring structure where the height of the edge of the dot is higher than the center of the structure (Figure 2C). The stability of

LbL dot arrays after printing was tested by storing LbL arrays in a pH 3.5 buffer solution for different periods of time up to 15 h. The dots were then monitored optically for any degradation or dissolution and with AFM for any changes in surface morphology (Figures 1 and 2). AFM images at different scales show relatively uniform surface morphology of the LbL dots even after prolonged exposure to the buffer solution (Figures 2, 3, S4, and S5, Supporting Information).

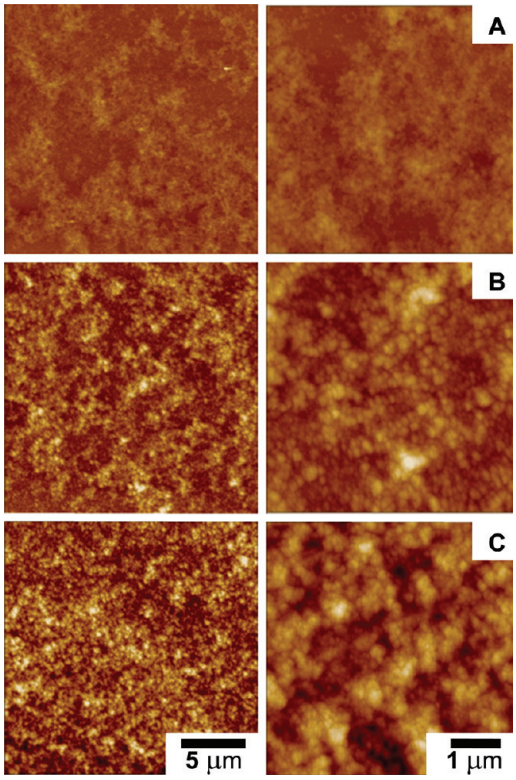

Figure 3. Higher resolution AFM images (left, 20 × 20 μm; right, 5 × 5 μm) displaying the surface morphology of LBL dots with (A) 1 bilayer, (B) 3 bilayers, and (C) 5 bilayers. The height is 200 nm for all images.

The AFM images demonstrate very consistent shape and dimensions of LbL dots at different locations and after different deposition cycles. The subsequent droplets, which are placed on the same position, are limited in spreading, and the overall diameter of the growing LbL dot remains confined to this initial size. The elevated height of the LbL dot edges after the initial deposition is a direct result of the coffee ring effect which occurs during the formation of the film and subsequent drying.[40−43] The evaporation of the polymer after deposition on a substrate created a capillary outward flow from the center of the film to the edge, which causes the formation of a characteristic coffee ring structure.[44−46] The coffee ring or doughnut-shaped structure indicates the early deposition of the polymer on the substrate during the evaporation process. This early deposition is the result of a high surface site density, a large equilibrium constant of the binding reaction, and a low interaction of polymer molecules in solutions.[47]

The AFM images demonstrate somewhat uneven surfaces associated with such a redistribution of polymer components during the droplets impact followed by solution drying with large-scale roughness (20 μm × 20 μm) ranging from 12 to 30 nm, still well below the average dot thickness.[48,49] The relatively smooth morphology is observed at higher magnification with modest domain surface texture associated with local domain formation caused by component aggregation as traditionally observed for hydrogen-bonded LbL films.[50−53] The microroughness at small scale surface areas (1 μm × 1 μm) is much lower, between 6 and 20 nm. This value corresponds to typical values previously observed for hydrogen-bonded planar LbL films[54] and LbL microcapsules.[55,56] The similarities in surface roughness indicate that LbL formation of microscopic dots with high-speed droplet delivery does not significantly alter the local morphology and microstructure from that of previously studied hydrogen-bonded LbL films and structures.

The thickness of the LbL dots increases dramatically with the number of depositions where the average thickness reaches 130 nm for 5 bilayers and 400 nm for 10 bilayers (with added intermediate dye component) (Figure 4). The average

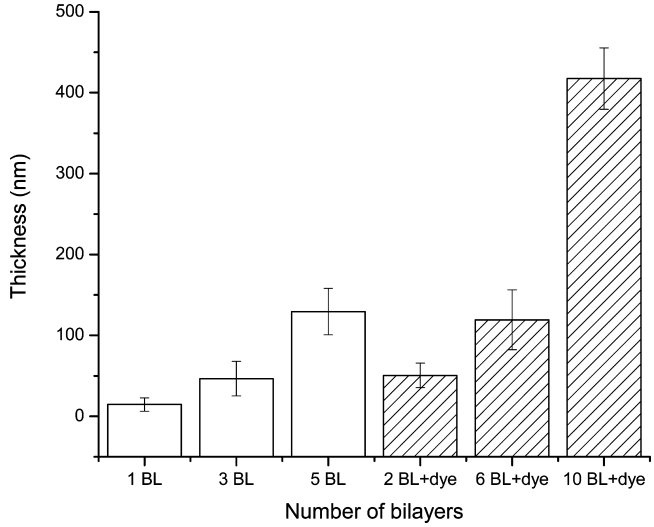

Figure 4. Thickness of LbL dots (empty) and LbL dye-encapsulated dots (dashed) vs number of bilayers. The error bars represent the average microroughness of each sample.

increment of the thickness growth is close to 40 nm per bilayer for the thicker dots. This thickness increment is much higher than thicknesses of other LbL films fabricated from similar components (around 4−6 nm per bilayer).[57−60] This difference in thickness growth rate might be caused by several important differences between inkjet-assisted LbL fabrication and traditional LbL assembly methods. First, it is apparent that the forced delivery of the components to the confined surface area during multiple depositions is limited by the initial spreading/dewetting of the aqueous solution on the hydrophobic substrate. This confinement results in the presence of an excess amount of material within the area surrounded by the elevated rim. Second, the absence of the washing step (common for traditional LbL depositions) causes an excess amount of polymer solution to stay within this limited surface area, thus promoting the formation of relatively uniform and thick additions of weekly bonded material. Third, we suggest that high interdiffusion of polymer chains into preformed swollen films can be promoted by both strong impact and high mobility of weakly bonded polymer components common for this type of LbL film.[61−63]

Next, the deposition of fluorescent dye in the center of the LbL dot followed by the capping polymer film with a different

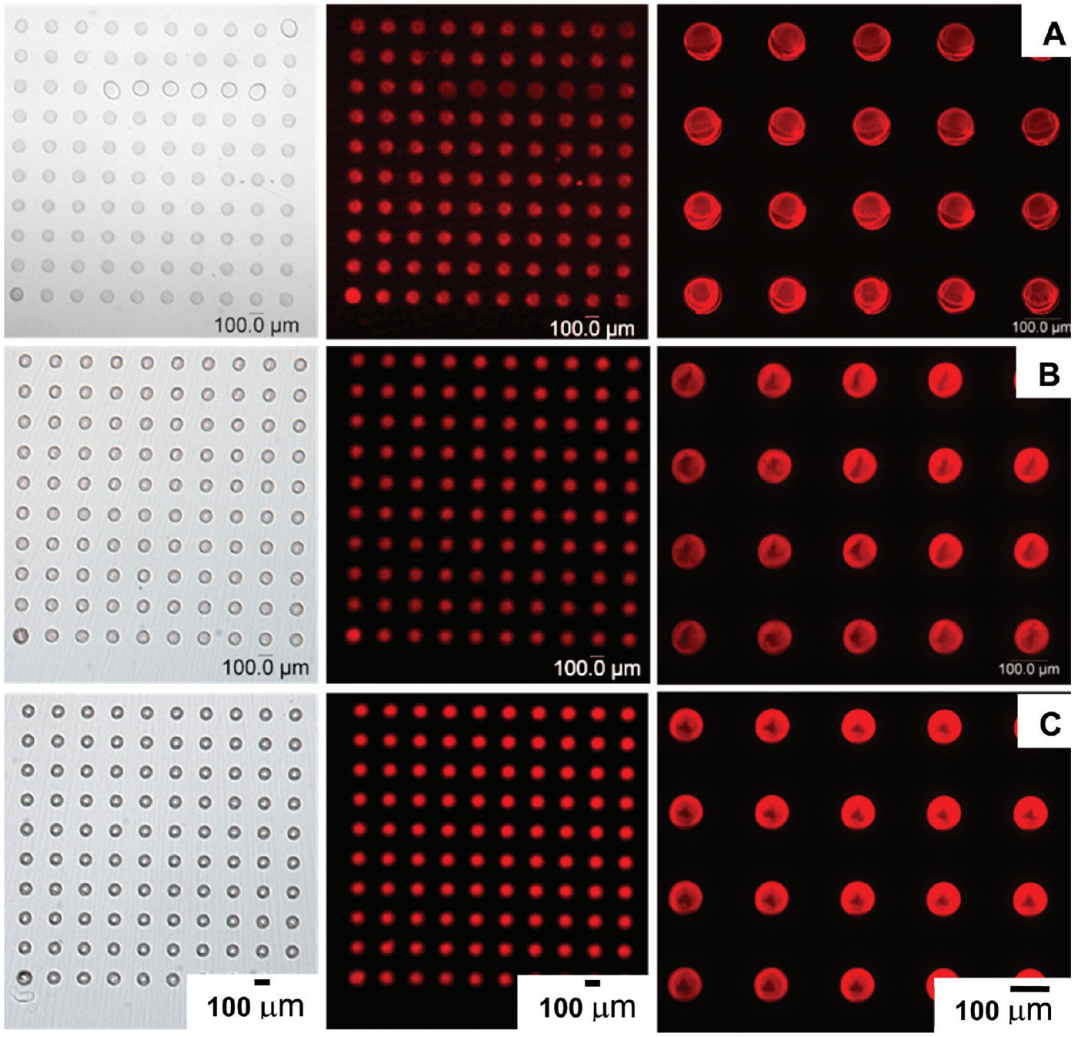

Figure 5. Optical and fluorescent images of 10 × 10 arrays of PVPON/PMAA LbL dots with encapsulated Rhodamine dye with different number of bilayers: (A) 2 bilayers, (B) 6 bilayers, and (C) 10 bilayers.

number of bilayers results in the uniform array of highly fluorescent dots which see the thickness increases to about 400 nm for 10 bilayer dots (Figure 4). The fluorescent images indicate the consistency of the printing process and the long-term stability of the encapsulation printing under an acidic buffer condition, even as the number of deposition cycles exceeds 6 (Figures 5, S6, and S7, Supporting Information). The average diameter of the printed dots is 82.4 ± 5.4 μm with the 50 μm diameter inkjet nozzles and remains virtually unchanged for different printing conditions and also after exposure to the buffer solution (Figure S8, Supporting Information).

AFM images show that, despite an overall uniform appearance, the central area of the dots seems to be depressed as indicated by reduced optical scattering, fluorescent intensity, and the overall elevation (Figure 6). We suggest that both confined spreading and impact at the central location result in such a nonuniform distribution of components after deposition. Also, the fluorescent dye might be partially redissolved and forced from the center of the dot after multiple depositions. The velocity of the droplets in our experiments was controlled between 1 and 3 m/s for the suitable printing conditions. This relatively high impact speed enhances spreading behavior of the polymer dot and induces coffee ring phenomena, which moves the fluorescent dye to the periphery and causes the formation of doughnut-shaped or coffee ring structure of the multilayer films. Such a coffee ring-like structure still remains visible for the thickest dots fabricated here (around 400 nm), but overall dot smoothing results in the central depression not exceeding 30−40% of the overall thickness (Figure 6). Increasing uniformity of the dots is observed with the increasing thickness through multiple layer depositions. For inkjet-assisted LbL encapsulation, the presence of the coffee ring structure might be desirable for better encapsulation results during following depositions compared to smooth film morphology. The coffee ring structure has an elevated wall at the periphery and lower cavity at the center of the structure. This morphology limits spreading behavior of the fluorescent dye toward to the rim of the structure and confines the dye inside the multilayer dots. As a result, the encapsulation efficiency of the fluorescent dye within the center of the LbL polymer dots increases for the coffee ring structure of LbL dots. These results demonstrate that capillary flow, central-area impact, and elevated rims play a significant role in the final morphology of the microscopic LbL dots.

AFM images confirm the stability of the inkjet-assisted LbL dye-encapsulated dots under long-term storage in acidic conditions. Only minor changes in the initial surface morphology and smoothing of the central depression are

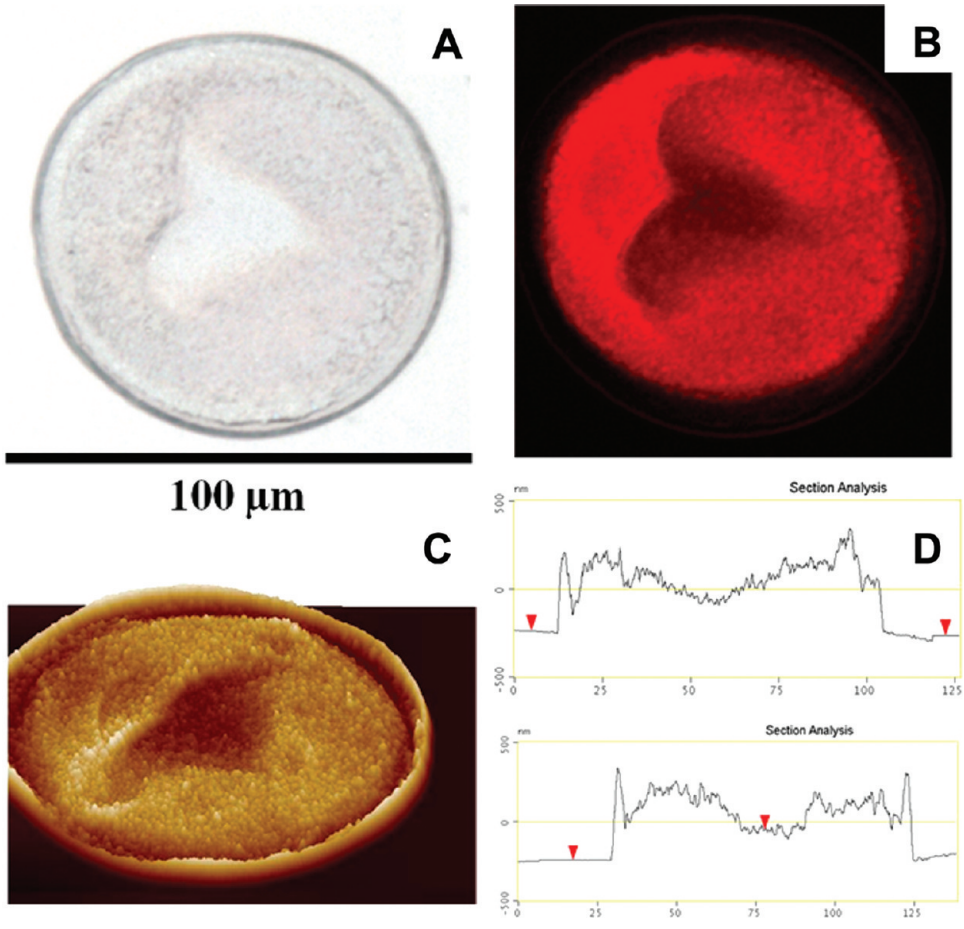

Figure 6. (A) Optical image, (B) fluorescence image, (C) 3D AFM image with *z*-scale of 2 μm, and (D) cross sections of 10 bilayer (5 + dye + 5) dots.

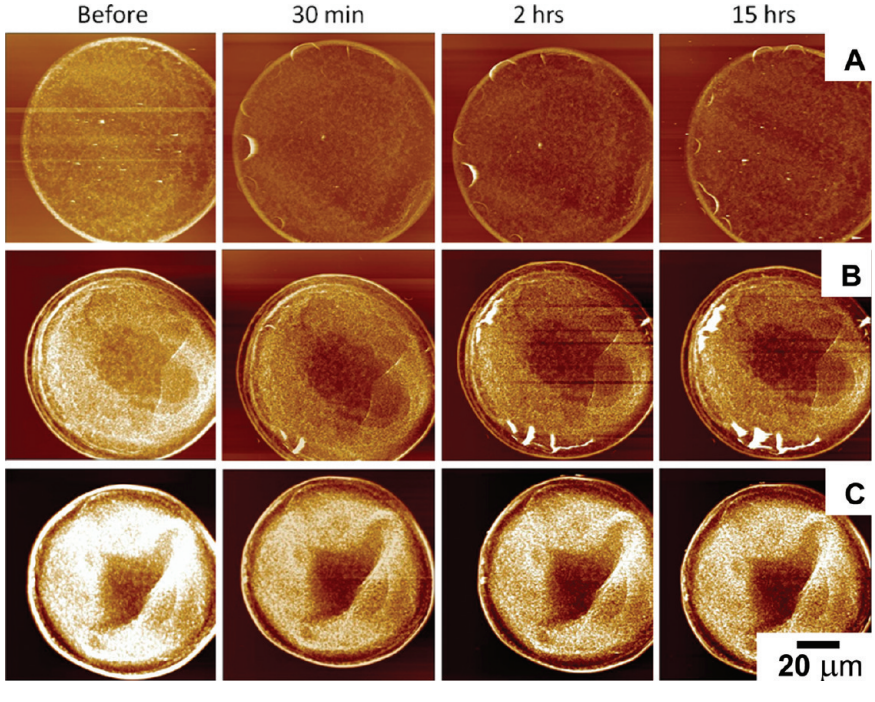

Figure 7. AFM images of LbL dye-encapsulated dots with different exposure times in buffer, pH 3.5: (A) 2 bilayers, (B) 6 bilayers, and (C) 10 bilayers. The image size is 100 μm, and the height is 500 nm for all images.

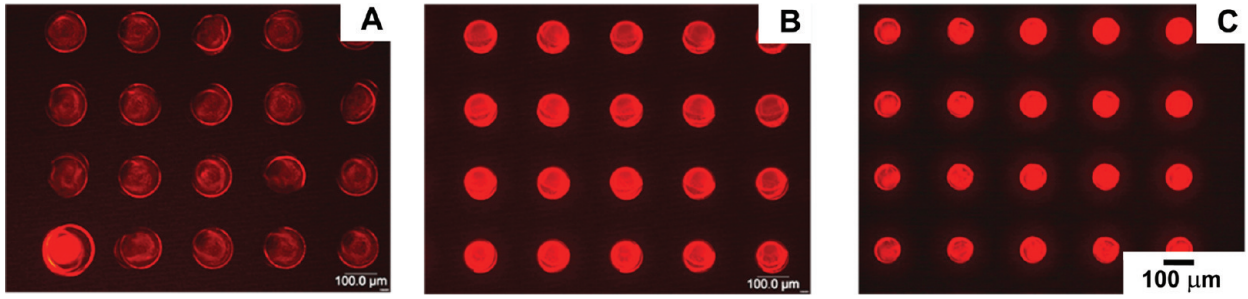

Figure 8. Fluorescent images of 2 bilayer LbL dye-encapsulated dot array on different substrates: (A) silicon, (B) PHS substrate, and (C) PS substrate. The printing process starts from the bottom left dot and ends at the top right spot.

observed (Figures 7, S9, and S10, Supporting Information). A minor reduction in the average thickness (5−15%) of the dots is observed after extended exposure to the acidic environment. The reduction in thickness is due to the dissolution of excess polymer, which remains in the structure since no rinsing step is used during fabrication to remove these unbound chains. The dots overall though show excellent stability of the hydrogen bonded polymer layers, even after extended exposure to an acidic environment (Figure S11, Supporting Information).

A direct comparison of various substrates is performed to assess the role of surface wettability and its impact on the inkjet-assisted LbL printing (Figure 8). The encapsulated dot arrays were printed on substrates with the following surface wetting properties: clean SiO_2 wafers (contact angle, 8°), PHS coated glass (contact angle, 71°), and PS coated glass slides (contact angle, 86°) (Figures S12 and S13, Supporting Information). As we observed, the smallest LbL dots formed on the hydrophilic surface with a diameter of 129 ± 3.5 μm, well exceeding the diameter of the deposited liquid droplet (50 μm). This sizable increase indicates major spreading of the polymer at the liquid−solid contact interface on the highly wettable surface. The size of the LbL dots decrease to 89 ± 2.4 and 82.4 ± 1.6 μm on PHS and PS substrates. The size of the dried polymer dot array depends on Weber number (We) and wettability of the polymer on the substrate. The highly spreading of the polymer droplet after printing on different substrates indicates high We, which agrees with common results from the inkjet system.[39,64] Additionally, the overall brightness and uniformity of the fluorescent array increase dramatically on the hydrophobic substrates (Figure 8).

For hydrophilic substrates, the Deegan flow is strongly developed in the polymer droplets. It moves the polymer and Rhodamine dye to the periphery and causes the coffee ring structure formation as mentioned in Figures 2 and 7. This coffee ring structure results in the uneven thickness of the multilayer dot with the thickness at the periphery much higher than the thickness at the center of the dot structure. However, this outward flow and coffee ring effect can be reduced by increasing the hydrophobicity of the substrate. In Figure 8, Rhodamine dye is shown to form a coffee ring structure when printed in a silicon substrate (contact angle, 8°). The spreading of the fluorescent dye and coffee ring formation are reduced when the dot is printed on a PHS substrate (contact angle, 71°) and the coffee ring is minimized for PS substrate (contact angle, 86°). Therefore, the hydrophobicity of the substrate can induce a uniform thickness of the LbL dots.

Finally, using the 20 μm diameter nozzle, the droplet size was reduced to 35 μm and the resulting printed LbL dot was measured at the smallest diameter of 37 μm on the hydrophobic PHS substrate, thus indicating very modest spreading of droplets upon impact. Using these substrates, we are able to fabricate features much smaller than those reported in earlier literature examples of LbL printing (around 100 μm) (Figure 9). This key observation indicates that the limiting factor in spatial resolution on a properly prepared substrate is the droplet size rather than the impact or spreading of the droplet on the nonwettable surface during printing. Hydrophobic surfaces, designed to reduce solution spreading, are an essential component of the printing process to achieve printing

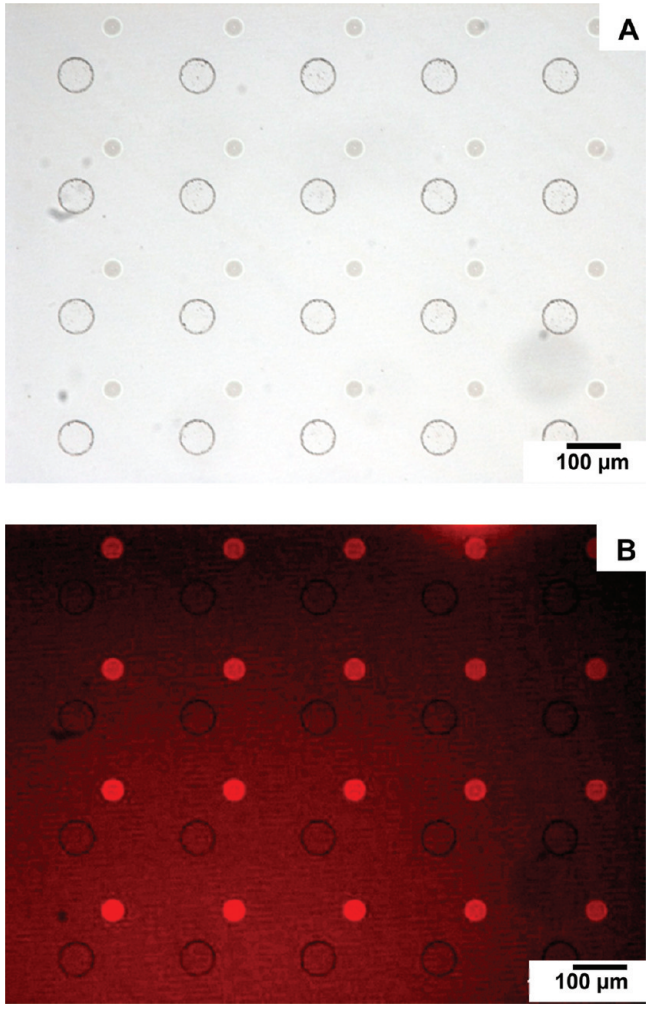

Figure 9. Optical (A) and fluorescence (B) images of an array of PVPON dots (large dots) and Rhodamine dots (small dots) printed from a 50 and a 20 μm nozzle, respectively.

of the smallest features possible. Thus, we suggest that the practical limit of inkjet-assisted LbL printing of polymer dots is about 10 μm, as this is the size of the smallest commercial nozzle available for commercial devices.

It is worth noting that a number of studies suggested that the evaporation rate and thermal annealing can affect the formation of the coffee ring structure, which can cause different encapsulation results.[18,65−68] However, in this study, we do not investigate the effect of solvents and the evaporation processes on the dot morphology because the overall focus of our studies on the encapsulation of water-based solutions appropriate for biomolecules and biological objects under ambient condition will be reported in forthcoming publications. Furthermore, the annealing process which can improve the stability and uniformity of the surface morphology cannot improve encapsulation efficiency because of the fluorescent dye.

Finally, to demonstrate versatility of this approach, we fabricated GT and inversed GT logos composed of fluorescent LbL dots on a PHS coated substrate using inkjet LbL printing to demonstrate the potential to create complicated patterns of dye-encapsulated dots (Figure 10). The Rhodamine solution was printed from a 20 μm diameter nozzle and showed well-resolved bright dots in the GT patterns (Figure 10). The dot size is around 35 μm, and the printing process can be completed within 20 s while retaining high patterning accuracy.

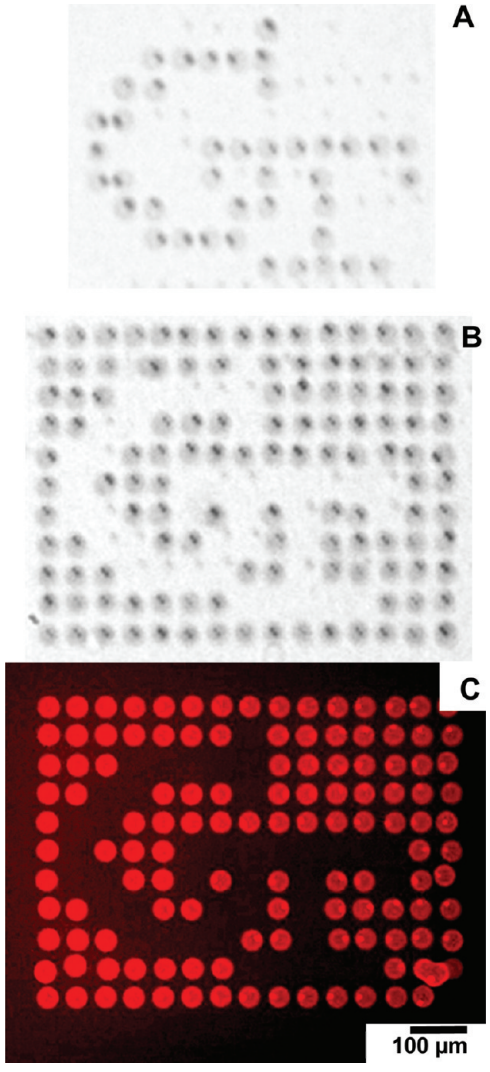

Figure 10. Optical (A, B) and fluorescent (C) image of inkjet-assisted LbL patterns: (A) GT logo and (B, C) inversed GT logo.

CONCLUSIONS

We have presented inkjet-assisted LbL printing of large-scale arrays of hydrogen-bonded polymeric dots and corresponding dye-encapsulated LbL dots. Microscopic dots with a controlled thickness ranging from 15 to 400 nm can be formed using PVPON/PMAA components with or without encapsulation of Rhodamine dye and while retaining a uniform patterned array on both hydrophilic and hydrophobic smooth substrates. We observe relatively uniform surface morphology of these polymer dots with a somewhat depressed central region caused by the droplet impact forcing the solution to flow toward the edges.

The minimum size of the LbL dots and, thus, the resolution of this method are dependent on the liquid droplet size as defined by the nozzle diameter as well as by the spreading behavior of the polymer solution on the different substrates. When the minimum nozzle diameter is employed on the non-wettable surfaces, inkjet-assisted LbL printing achieved a minimum spatial resolution of below 40 μm, which is a significant improvement, compared to obtainable feature sizes prior to the use of inkjet LbL printing. We suggest that these arrays of polymer dots can be utilized to encapsulate a variety of different components by delivering small liquid droplets to the central area and further capping them with additional polymer multilayers.

Inkjet-assisted LbL printing is a fast and simple method of complex array formation without the use of an intermediate washing step and no sacrificial solid core template to support the layered formation. Inkjet-assisted LbL printing allows direct payload delivery in a continuous process enabling the formation of large, complex and high resolution arrays of multiple materials. These large-scale arrays of organized LbL microdots have potential for various applications in diagnostics, cellular mechanobiology, and therapeutic and biosensing applications if controlled loading and unloading of payload is required.[69,70] We suggest that inkjet-assisted encapsulation provides apparent advantages over conventional LbL encapsulation in uniform ultrathin films and microcapsules due to its efficient, facile, and flexible fabrication process over large areas.

ASSOCIATED CONTENT

Supporting Information

Additional figures. This information is available free of charge via the Internet at http://pubs.acs.org/.

AUTHOR INFORMATION

Corresponding Author

*E-mail: vladimir@mse.gatech.edu.

Notes

The authors declare no competing financial interest.

ACKNOWLEDGMENTS

The authors thank David S. Gottfried, Andrew P. Shaw, and Kyle D. Anderson for technical assistance. Funding from the FA9550-11-1-0233 and FA9550-09-1-0162 (BIONIC Center) Projects from Air Force Office Of Scientific Research (printing), by the U.S. Department of Energy, Office of Basic Energy Sciences, Division of Materials Sciences and Engineering under Award # DE-FG02-09ER46604 (LbL assembly), and

SCG Paper PLC (Fellowship for RS) are gratefully acknowledged.

REFERENCES

(1) Decher, G.; Schlenoff, J. B.; Lehn, J.-M. *Multilayer Thin films:Sequential Assembly of Nanocomposite materials*; WILEY-VCH: Weinheim, 2003.
(2) Tsukruk, V. V. *Prog. Polym. Sci.* **1997**, *22*, 247−311.
(3) Lvov, Y.; Möhwald, H. *Protein Architecture: Interfacial Molecular Assembly and Immobilization Biotechnology*; Marcel Dekker, New York, 2000.
(4) Hammond, P. T. *Adv. Mater.* **2004**, *16*, 1271−1293.
(5) Stuart, M. C.; Huck, W.; Genzer, J.; Müller, M.; Ober, C.; Stamm, M.; Sukhorukov, G.; Szleifer, I.; Tsukruk, V. V.; Urban, M.; Winnik, F.; Zauscher, S.; Luzinov, I.; Minko, S. *Nat. Mater.* **2010**, *9*, 101−113.
(6) Ko, H.; Jiang, C.; Tsukruk, V. V. *Chem. Mater.* **2005**, *17*, 5489−5497.
(7) Zhao, W.; Xu, J.-J.; Shi, C.-G.; Chen, H.-Y. *Langmuir* **2005**, *21*, 9630−9634.
(8) Kotov, N. A.; Dékány, I.; Fendler, J. H. *Adv. Mater.* **1996**, *8*, 637−641.
(9) Zheng, H.; Lee, I.; Rubner, M. F.; Hammond, P. T. *Adv. Mater.* **2002**, *14*, 569−572.
(10) Kinnane, C. R.; Such, G. K.; Caruso, F. *Macromolecules* **2011**, *44*, 1194−1202.
(11) Sukhishvili, S. A. *Curr. Opin. Colloid Interface Sci.* **2005**, *10*, 37−44.
(12) Zhang, H.; Fu, Y.; Wang, D.; Wang, L.; Wang, Z.; Zhang, X. *Langmuir* **2003**, *19*, 8497−8502.
(13) Ariga, K.; Ji, Q.; Hill, J. P. *Adv. Polym. Sci.* **2010**, *229*, 51−87.
(14) Choi, J.; Rubner, M. F. *Macromolecules* **2005**, *38*, 116−124.
(15) Jiang, C.; Tsukruk, V. V. *Adv. Mater.* **2006**, *18*, 829−840.
(16) Caruso, F.; Susha, A. S.; Giersig, M.; Mohwald, H. *Adv. Mater.* **1999**, *11*, 950−953.
(17) deGans, B. J.; Duineveld, P. C.; Schubert, U. S. *Adv. Mater.* **2004**, *16*, 203−213.
(18) Singh, M.; Haverinen, H. M.; Dhagat, P.; Jabbour, G. E. *Adv. Mater.* **2010**, *22*, 673−685.
(19) Gates, B. D.; Xu, Q.; Stewart, M.; Ryan, D.; Willson, C. G.; Whitesides, G. M. *Chem. Rev.* **2005**, *105*, 1171−1196.
(20) Whitesides, G. M.; Ostuni, E.; Takayama, S.; Jiang, X.; Ingber, D. E. *Annu. Rev. Biomed. Eng.* **2001**, *3*, 335−373.
(21) Xia, Y.; Whitesides, G. M. *Angew. Chem., Int. Ed.* **1998**, *37*, 550−575.
(22) Jiang, X.; Zheng, H.; Gourdin, S.; Hammond, P. T. *Langmuir* **2002**, *18*, 2607−2615.
(23) Quist, A. P.; Pavlovic, E.; Oscarsson, S. *Anal. Bioanal. Chem.* **2005**, *381*, 591−600.
(24) Heckele, M.; Schomburg, W. K. *J. Micromech. Microeng.* **2004**, *14*, R1−R14.
(25) Piner, R. D.; Zhu, J.; Xu, F.; Hong, S.; Mirkin, C. A. *Science* **1999**, *28*, 661−663.
(26) Lavalle, P.; Voegel, J.-C. *Adv. Mater.* **2011**, *23*, 1191−1221.
(27) Schaaf, P.; Voegel, J.-C.; Jierry, L.; Boulmedais, F. *Adv. Mater.* **2012**, *24*, 1001−1016.
(28) Calvert, P. *Chem. Mater.* **2001**, *13*, 3299−3305.
(29) Tekin, E.; Smith, P. J.; Schubert, U. S. *Soft Matter* **2008**, *4*, 703−713.
(30) Park, J.-U.; Hardy, M.; Kang, S. J.; Barton, K.; Adair, K.; Mukhopadhyay, D. K.; Lee, C. Y.; Strano, M. S.; Alleyne, A. G.; Georgiadis, J. G.; Ferreira, P. M.; Rogers, J. A. *Nat. Mater.* **2007**, *6*, 782−789.
(31) Yang, S. Y.; Rubner, M. F. *J. Am. Chem. Soc.* **2002**, *124*, 2100−2101.
(32) Andres, C, M.; Kotov, N. A. *J. Am. Chem. Soc.* **2010**, *132*, 14496−14502.
(33) Derby, B. *Annu. Rev. Mater. Res.* **2010**, *40*, 395−414.
(34) Szunerits, S.; Boukherroub, R. *Langmuir* **2006**, *22*, 1660−1663.
(35) Sheller, N. B.; Petrash, S.; Foster, M. D.; Tsukruk, V. V. *Langmuir* **1998**, *14*, 4535−4544.
(36) Tsukruk, V. V.; Bliznyuk, V. N. *Langmuir* **1998**, *14*, 446−455.
(37) Tsukruk, V. V.; Reneker, D. H. *Polymer* **1995**, *36*, 1791−1808.
(38) McConney, M. E.; Singamaneni, S.; Tsukruk, V. V. *Polym. Rev.* **2010**, *50*, 235−286.
(39) Son, Y.; Kim, C.; Yang, D. H.; Ahn, D. J. *Langmuir* **2008**, *24*, 2900−2907.
(40) Deegan, R. D.; Bakajin, O.; Dupont, T. F.; Huber, G.; Nagel, S. R.; Witten, T. A. *Nature* **1997**, *389*, 827−829.
(41) Soltman, D.; Subramanian, V. *Langmuir* **2008**, *24*, 2224−2231.
(42) Sharma, V.; Park, K.; Srinivasarao, M. *Mater. Sci. Eng., R* **2009**, *65*, 1−38.
(43) Xu, J.; Xia, J.; Hong, S. W.; Lin, Z.; Qiu, F.; Yang, Y. *Phys. Rev. Lett.* **2006**, *96*, 066104−066108.
(44) Shen, X.; Ho, C.-M.; Wong, T.-S. *J. Phys. Chem. B* **2010**, *114*, 5269−5274.
(45) Weon, B. M.; Je, J. H. *Phys. Rev. E* **2010**, *82*, 015305−4.
(46) Hong, S. W.; Jeong, W.; Ko, H.; Kessler, M. R.; Tsukruk, V. V.; Lin, Z. *Adv. Funct. Mater.* **2008**, *18*, 2114−2122.
(47) Kim, H. Y.; Lee, S. E.; Kim, M. J.; Han, J. I.; Kim, B. K.; Lee, Y. S.; Lee, Y. S.; Kim, J. H. *BMC Bioinf.* **2007**, *8*, 485−496.
(48) Choi, I.; Suntivich, R.; Plamper, F. A.; Synatschke, C. V.; Mueller, A. H. E.; Tsukruk, V. V. *J. Am. Chem. Soc.* **2011**, *133*, 9592−9606.
(49) Stockton, W. B.; Rubner, M. F. *Macromolecules* **1997**, *30*, 2717−2725.
(50) Kharlampieva, E.; Kozlovskaya, V.; Chan, J.; Ankner, J. F.; Tsukruk, V. V. *Langmuir* **2009**, *25*, 14017−14024.
(51) Kozlovskaya, V.; Kharlampieva, E.; Chang, S.; Muhlbauer, R.; Tsukruk, V. V. *Chem. Mater.* **2009**, *21*, 2158−2167.
(52) Lisunova, M. O.; Drachuk, I.; Shchepelina, O. A.; Anderson, K.; Tsukruk, V. V. *Langmuir* **2011**, *27*, 11157−11165.
(53) Kozlovskaya, V.; Harbaugh, S.; Drachuk, I.; Shchepelina, O.; Kelley-Loughnane, N.; Stone, M.; Tsukruk, V. V. *Soft Matter* **2011**, *7*, 2364−2372.
(54) Kharlampieva, E.; Kozlovskaya, V.; Ankner, J. F.; Sukhishvili, S. A. *Langmuir* **2008**, *24*, 11346−11349.
(55) Kharlampieva, E.; Kozlovskaya, V.; Sukhishvili, S. A. *Adv. Mater.* **2009**, *21*, 3053−3065.
(56) Kozlovskaya, V.; Kharlampieva, E.; Drachuk, I.; Cheng, D.; Tsukruk, V. V. *Soft Matter* **2010**, *6*, 3596−3608.
(57) Zhuk, A.; Pavlukhina, S.; Sukhishvili, S. A. *Langmuir* **2009**, *25*, 14025−14029.
(58) Sukhishvili, S. A.; Granick, S. *Macromolecules* **2002**, *35*, 301−310.
(59) Kozlovskaya, V. A.; Kharlampieva, E. P.; Erel-Unal, I.; Sukhishvili, S. A. *Polym. Sci. Ser. A* **2009**, *51*, 719−729.
(60) Sukhishvili, S. A.; Granick, S. *J. Am. Chem. Soc.* **2000**, *122*, 9550−9551.
(61) Seo, J.; Lutkenhaus, J. L.; Kim, J.; Hammond, P. T.; Char, K. *Langmuir* **2008**, *24*, 7995−8000.
(62) Podsiadlo, P.; Michel, M.; Lee, J.; Verploegen, E.; Kam, N. W. S.; Ball, V.; Lee, J.; Qi, Y.; Hart, A. J.; Hammond, P. T.; Kotov, N. A. *Nano Lett.* **2008**, *8*, 1762−1770.
(63) Dubas, S. T.; Schlenof, J. B. *Macromolecules* **1999**, *32*, 8153−8160.
(64) Son, Y.; Kim, C. *J. Non-Newtonian Fluid Mech.* **2009**, *162*, 78−87.
(65) Lim, J. A.; Lee, W. H.; Lee, H. S.; Lee, J. H.; Park, Y. D.; Cho, K. *Adv. Funct. Mater.* **2008**, *18*, 229−234.
(66) Li, Y.; Fu, C.; Xu, J. *Jpn. J. Appl. Phys.* **2007**, *46*, 6807−6810.
(67) Yunker, P. J.; Still, T.; Lohr., M. A.; Yodh, A. G. *Nature* **2011**, *476*, 308−311.
(68) Soltman, D.; Subramanian, V. *Langmuir* **2008**, *24*, 2224−2231.
(69) Xu, T.; Kincaid, H.; Atala, A.; Yoo, J. J. *J. Manuf. Sci. Eng.* **2008**, *130*, 021017−021015.
(70) Poellmann, M. J.; Barton, K. L.; Mishra, S.; Johnson, A. J. W. *Macromol. Biosci.* **2011**, *11*, 1164−1168.